Communication

Highly Photostable and Fluorescent Microporous Solids Prepared via Solid-state Entrapment of BODIPY Dyes in a Nascent Metal-Organic Framework

Viktorija Glembockyte, Mathieu Frenette, Cristina Mottillo, Andres M. Durantini, Jeff Gostick, Vjekoslav Strukil, Tomislav Friscic, and Gonzalo Cosa

J. Am. Chem. Soc., **Just Accepted Manuscript** • Publication Date (Web): 21 Nov 2018

Highly Photostable and Fluorescent Microporous Solids Prepared via Solid-state Entrapment of BODIPY Dyes in a Nascent Metal-Organic Framework

Viktorija Glembockyte[1], Mathieu Frenette[1,2], Cristina Mottillo[1], Andrés M. Durantini [1,4], Jeff Gostick[3], Vjekoslav Štrukil[1,5], Tomislav Friščić[1,5]* and Gonzalo Cosa[1]*

[1]Department of Chemistry and Quebec Centre for Applied Materials (QCAM), McGill University, 801 Sherbrooke St. W., Montreal, QC, Canada, H3A 0B8; [2]Department of Chemistry, Université du Québec à Montréal, Case postale 8888, Succursale Centre-Ville, Montreal, QC, Canada H3C 3P8; [3]Department of Chemical Engineering, McGill University, 3610 University Street, Montreal, QC, Canada; [4]Departamento de Química, Facultad de Ciencias Exactas, Físico-Químicas y Naturales, Universidad Nacional de Río Cuarto, Ruta Nacional 36 Km 601, X5804BYA Río Cuarto, Córdoba, Argentina; [5]Ruđer Bošković Institute, Bijenička cesta 54,10000 Zagreb, Croatia

Supporting Information Placeholder

ABSTRACT: We report a strategy to synthesize highly emissive, photostable, microporous materials by solid-state entrapment of boron dipyrromethene (BODIPY) fluorophores in a metal-organic framework. Solvent-free mechanochemistry or accelerated aging enabled quantitative capture and dispersal of the PM605 dye within the ZIF-8 framework starting from inexpensive, commercial materials. While the design of emissive BODIPY solids is normally challenged by quenching in a densely-packed environment, herein reported PM605@ZIF-8 materials show excellent emissive properties and to the best of our knowledge an unprecedented ~10-fold enhancement of BODIPY photostability. Time-resolved and steady-state fluorescence studies of PM605@ZIF-8 show that interchromophore interactions are minimal at low dye loadings, but at higher ones lead to through-pore energy transfer between chromophores and to aggregate species.

Organic solid-state fluorescent materials are increasingly sought after for developing optoelectronic devices,[1-2] such as lasers,[3-4] data recording and storage devices,[5-6] and sensors.[7-9] A major hurdle in using readily available organic fluorophores for such applications is in the reduced photon output due to aggregation-caused quenching, [10-11] typically resulting from non-emissive H-aggregate formation in densely-packed chromophores. While boron dipyrromethene (BODIPY) dyes[12] exhibit high absorptivity and fluorescent quantum yields, long singlet excited state lifetimes, and tunable emissions, their use as solid-state fluorescent materials is prevented by rapid quenching in a crystalline solid (see Figure S1), facilitated by intrinsic planarity and preference for π-stacking.[13] Strategies to mitigate such undesired molecular interactions have so far focused on modification of the chromophore to prevent formation of ordered structures,[14-23] induce the formation of emissive J-aggregates,[24-27] or diluting the BODIPY fluorophores in a polymer matrix.[28-31]

Here we present an efficient strategy to synthesize highly fluorescent, photostable and microporous BODIPY-based materi-als, by solvent-free entrapment of the dye in a metal-organic framework (MOF)[32] being assembled by mechanochemistry[33-34] or "accelerated aging" (Figure 1).[35-36] By using the popular zinc 2-methylimidazolate Zn(**MeIm**)$_2$ (ZIF-8)[37-41] as the host MOF,[42-44] we show that the quantitative uptake of the commercial BODIPY dye PM605 during solid-state MOF assembly results in excellent emission properties. Most importantly, entrapment lead to an unprecedented ~10-fold enhancement in BODIPY photostability. Notably, because solvent-free routes enable rapid assembly of ZIF-8 from ZnO,[45] this strategy offers a clean, rapid route to photostable, emissive materials from the simplest, inexpensive components.

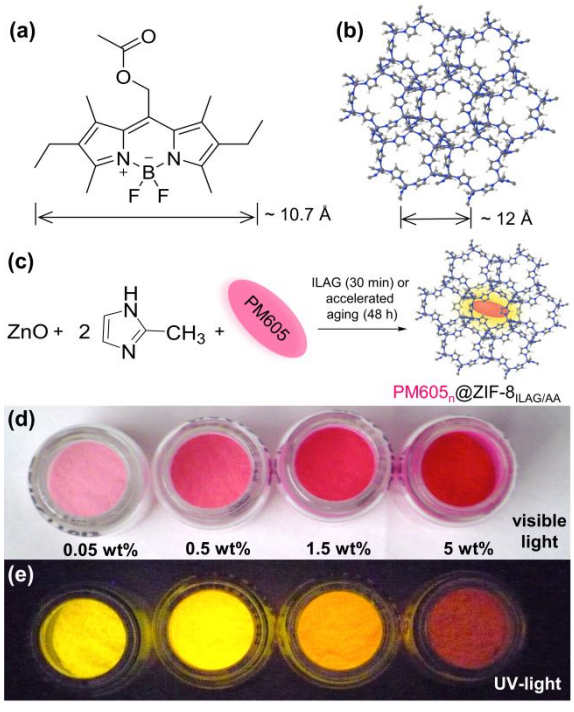

Figure 1. Structures of (a) PM605 and (b) ZIF-8; (c) herein des-cribed solid-state mechanochemical or accelerated aging syntheses of PM605$_n$@ZIF-8 materials. Selected PM605$_n$@ZIF-

8_{ILAG} samples viewed under: (d) room light and (e) ultraviolet light (centered at 350 nm).

Our strategy is based on comparing the pore and channel sizes of ZIF-8 (Figure 1) to molecular dimensions of PM605. The maximum diameter of a ZIF-8 pore is ca. 12 Å, sufficient to host a PM605 molecule whose longest dimension is ca. 11 Å. However, ZIF-8 pores are connected by channels of only 3.4 Å in diameter, which means that any PM-605 molecules inserted into the pore should be permanently trapped. At the same time, this also indicates that the BODIPY dye could not be readily introduced into ZIF-8 by simple soaking[46-49] of the pre-synthesized MOF in a solution of the dye.[50-51] Consequently, in order to introduce the dye into ZIF-8, we turned to synthesizing the framework in the presence of guests,[52-53] which should lead to *in situ* entrapment of the dye in the pores of the MOF as it is being formed. To maximize the efficiency of such a strategy, we explored dye entrapment in a solvent-free process, in that way avoiding the dispersion of the dye in a large volume of solvent. Notably, ZIF-8 readily forms from a 1:2 stoichiometric mixture of ZnO and 2-methylimidazole (**HMeIm**) in the presence of a protic catalyst either mechanochemically, by milling in the presence of a liquid additive (ion-and liquid-assisted grinding, ILAG), or by accelerated aging, *i.e.* by exposure to high relative humidity (RH) and mild temperature (45 °C). Consequently, we speculated that adding PM-605 dye to the corresponding solid-state reaction mixtures would enable the direct conversion of ZnO into PM605@ZIF-8 composites, with the PM605 dye permanently trapped within the MOF.

The formation of pink-colored materials was indeed observed upon ILAG[33] (Figure 1d) or accelerated aging[35-36] of 1:2 stoichiometric mixtures of ZnO and **HMeIm** in the presence of 0.05-5.0% weight content of solid PM605 ($PM605_n$@$ZIF\text{-}8_{ILAG}$ and $PM605_n$@$ZIF\text{-}8_{AA}$, respectively, *n* represents the percent weight content of dye). While solid PM605 does not exhibit noticeable fluorescence in the solid state (Figure S1), $PM605_n$@ZIF-8 materials were highly emissive, consistent with dye dispersal in the framework (Figure 1e). That PM605 was permanently trapped in ZIF-8, rather than adsorbed on the external surface, was verified by retention of color and emissive properties of the materials after multiple washings with methanol (MeOH) and dichloromethane (DCM). Quantifying the amount of PM605 in the washing supernatant indicated a dye encapsulation efficiency of 96-100% for $PM605_n$@$ZIF\text{-}8_{ILAG}$ and 73-93% for $PM605_n$@$ZIF\text{-}8_{AA}$ (Table S1)

Formation of ZIF-8 by ILAG and accelerated aging was confirmed by powder X-ray diffraction (PXRD) patterns of all prepared PM605@ZIF-8 materials, which demonstrated an excellent match to the simulated pattern of ZIF-8 (CSD code VELVOY) (Figures 2a, S2). The materials also exhibited a high porosity, as exemplified by BET surface areas for $PM605_{0.05}$@$ZIF\text{-}8_{ILAG}$ and $PM605_{0.05}$@$ZIF\text{-}8_{AA}$ of 1522 $m^2\ g^{-1}$ and 1605 $m^2\ g^{-1}$, respectively, after washing with MeOH and evacuation (Figures 2b-c). These surface areas are comparable with those previously reported for ZIF-8, consistent with the low loading of the dye (highest concentration of PM605 involved ~7%, pore occupancy, see also Table S1).[33, 44, 54-61]

Photophysical properties of $PM605_n$@ZIF-8 samples were evaluated by measuring emission (Figure 3a and Figure S3-S5), excitation (Figure S6) and Uv-VIS diffuse reflectance (Figure S7) spectra as well as fluorescence emission quantum yields (ϕ_f, Table S2) and fluorescence lifetimes (Figure 3b, and Figure S8). Bi-exponential fluorescence decays were seen for all ILAG samples (Table S3), indicating at least two distinct dye environments.

The emission properties of the lowest-loading $PM605_{0.05}$@$ZIF\text{-}8_{ILAG}$ are superior to those of PM605 in solution. For example, $PM605_{0.05}$@$ZIF\text{-}8_{ILAG}$ exhibits a slightly higher average fluorescence lifetime τ_{avg}=7.5 ns, compared to dilute acetonitrile solutions exhibiting a mono-exponential decay with τ=6.76 ns[62] (see also SI). The increased fluorescence lifetime highlights a drop in the nonradiative decay rate upon incarceration of PM605 in the MOF, possibly a result of the rigid surroundings. As the MOF should not affect the radiative decay lifetime of the dye (~10 ns),[62] the data reveals that PM605 emission quantum yield in the MOF is higher than in acetonitrile solution (ϕ_f = 0.67).[62] Values for ϕ_f of 0.68 in MOF were recorded for $PM605_{0.05}$@$ZIF\text{-}8_{ILAG}$ (see Table S2).

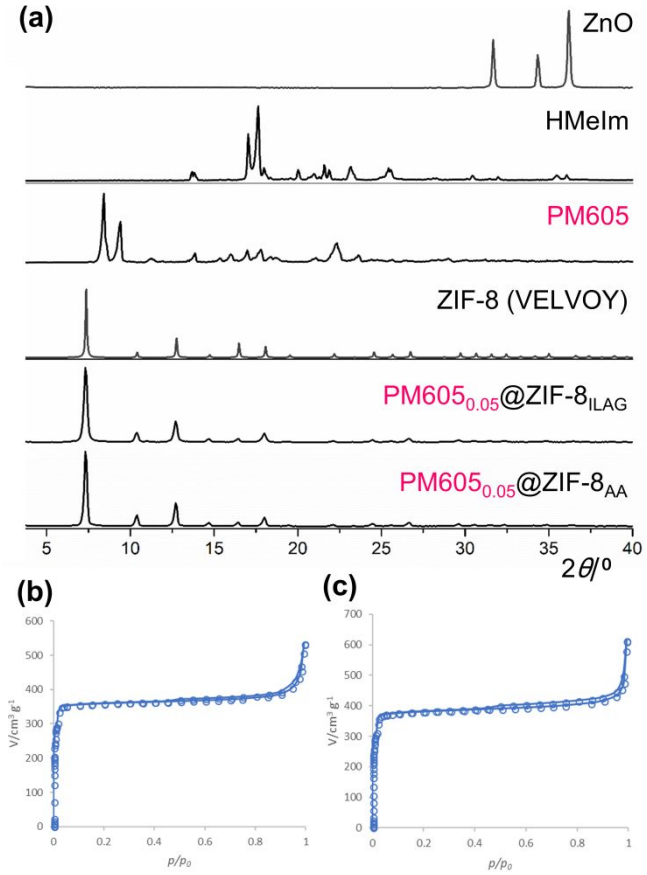

Figure 2. (a) Selected PXRD patterns for: ZnO, **HMeIm**, solid PM605, simulated for ZIF-8 (CSD code VELVOY), $PM605_{0.05}$@$ZIF\text{-}8_{ILAG}$ and $PM605_{0.05}$@$ZIF\text{-}8_{AA}$. Comparison of N_2 sorption experiments for (b) $PM605_{0.05}$@$ZIF\text{-}8_{ILAG}$ and (c) $PM605_{0.05}$@$ZIF\text{-}8_{AA}$.

Photophysical properties of $PM605_n$@$ZIF\text{-}8_{ILAG}$ were highly dependent on dye loading. Increasing the PM605 content from 0.05 to 0.5 wt% led to increased emission, consistent with a higher pore occupancy of the dye (Figure 3a-b) albeit there was a drop in ϕ_f from 0.68 to 0.40 respectively. Even higher loadings (up to 5.0 wt%) led to fluorescence intensity quenching (ϕ_f = 0.28 and 0.08 for 1.5% and 5% wt loading, respectively), reduced fluorescence lifetimes (Figures 3a-b, Table S2), the appearance of a higher energy band in the excitation and diffuse reflectance spectra (Figures S6 and S7),

and red-shifted emission (Figures 3a, S4), all indicative of interchromophore interactions, either within pore or through pore. These results are consistent with formation of non-emissive or weakly emissive H-aggregates that, we postulate, arise from double pore occupancy with increased dye loading (0.05 to 0.5, 1.5 and 5 wt% loading lead to estimated pore occupancies of 0.07, 0.7, 2.2 and 7%, respectively). No appreciable emission was obtained from control samples prepared either with ZIF-8_{ILAG} or ZIF-8_{AA} and lacking PM605 (Figure 3a).

Consistent with energy migration between fluorophores in different ZIF-8 pores, time-resolved fluorescence studies of PM605@ZIF-8_{ILAG} samples showed a gradual shortening of fluorescence lifetimes (Figure 3b) with increasing (1.5% wt or higher) PM605 load. The results highlight that dynamic - through-pore - energy transfer process to non-emissive or partially emissive aggregates (e.g. dimers within a pore) takes place at high dye loading. BODIPY dyes have a small Stokes shift favoring efficient homo energy transfer. Energy transfer between neighbouring PM605 molecules to lower energy "trap sites" (e.g. PM605 aggregates) is consistent with the red-shift in fluorescence emission observed with increasing concentration of PM605 in the ZIF-8 framework (Figures 3a and S4).

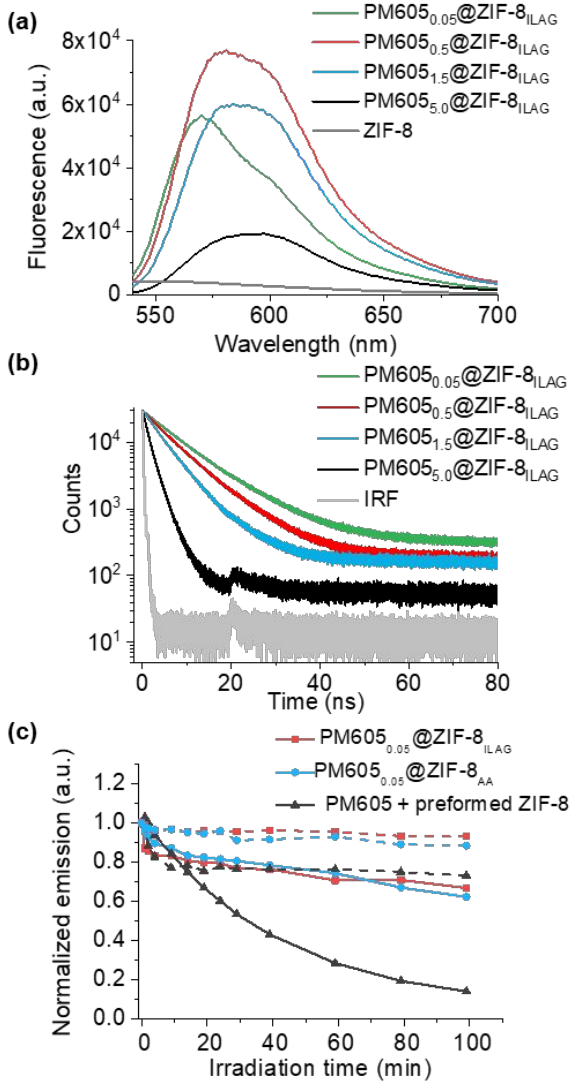

Figure 3. (a) Fluorescence emission spectra for PM605@ZIF-8_{ILAG} samples upon excitation at 520 nm and (b) Fluorescence lifetimes obtained upon exciting the samples at 467 nm and monitoring their emission at 590 nm. (c) Normalized integrated emission of PM605$_{0.05}$@ZIF-8_{ILAG} and PM605$_{0.05}$@ZIF-8_{AA} samples and free PM605 in ZIF-8 containing acetonitrile monitored after different irradiation times (solid lines). The extent of PM605 degradation due to photobleaching can be estimated by comparing the fluorescence intensity obtained to that of dark control samples (dashed lines).

The PM605@ZIF-8_{AA} solids displayed a similar inverse relationship between loading and emission intensity (Figure S5a), with PM605$_{0.5}$@ZIF-8_{AA} being the most emissive. However, in most cases the emission intensity of PM605@ZIF-8_{AA} samples was lower than for analogous PM605@ZIF-8_{ILAG} ones (Figure S5b). Furthermore, the fluorescence decays of PM605@ZIF-8_{AA} samples followed a multi-exponential decay model and were less sensitive to PM605 loading (Figure S8), suggesting a rather heterogeneous fluorophore distribution in the pores.

The PM605$_n$@ZIF-8 solids exhibited dramatically enhanced photostability, as revealed by comparing the rate of photobleaching for a PM605$_{0.05}$@ZIF-8_{ILAG} sample dispersed in acetonitrile to that of a control sample containing an equivalent amount of ZIF-8 dispersed in an acetonitrile solution of PM605. Recording the fluorescence spectra of the samples after different exposure times to blue LED light (450±25 nm, 180 mW cm^{-2}) (Figure 3c, solid lines) and comparison to control samples kept in the dark (Figure 3c, dashed lines) revealed rapid photobleaching of free PM605 in acetonitrile. Following 100 min of irradiation only ~15% of the initial fluorescence intensity remained (Figures 3c, S9-10). In contrast, photobleaching was significantly lower for PM605$_n$@ZIF-8 samples where 70% to 80% of the initial intensity was observed after 100 min irradiation (Figures 3c, S9-10). Based on the initial rates of photodegradation obtained once samples equilibrated, entrapment of the dye within the ZIF-8 porous structure enhanced its photostability by ~10-fold. A sudden intensity drop was observed with both dark controls and irradiated samples which we assign to particle aggregation and increased scattering upon solvent addition.

The enhanced photostability of PM605 within ZIF-8 may be due to partial shielding of the dye excited state by the framework, with reduced molecular mobility and hindered encounters with solvent and/or O_2 molecules minimizing the rates of photochemical (*e.g.* rearrangements) and photophysical (*e.g.* sensitization of singlet oxygen followed by chromophore oxidation) processes related to dye photobleaching.[63] Similar mechanisms have been suggested for dyes complexed to supramolecular hosts[64-65] or linked to dendrimers.[66-70]

In summary, we have demonstrated how solvent-free, solid-state chemistry enables the efficient preparation of microporous and fluorescent solids with highly enhanced photostability of a BODIPY dye, starting from simple, readily available components. This approach led to the first examples of highly stable solid-state fluorescent materials based on BODIPY dyes. Our approach provides an efficient alternative to the recently reported inclusion of fluorophores and nanoparticles within MOF[54, 71] upon crystallizing the framework from a solution of dissolved or dispersed guests. By avoiding the need for covalent modification of the

fluorophore, this approach also enables the preservation of the electronic properties of the dye and makes the approach readily extendable to other dyes of suitable molecular size. Preliminary work shows that this strategy can be used with other BODIPY systems, yielding highly fluorescent solids with emission properties spanning the entire 500–800 nm window (Figure 4).

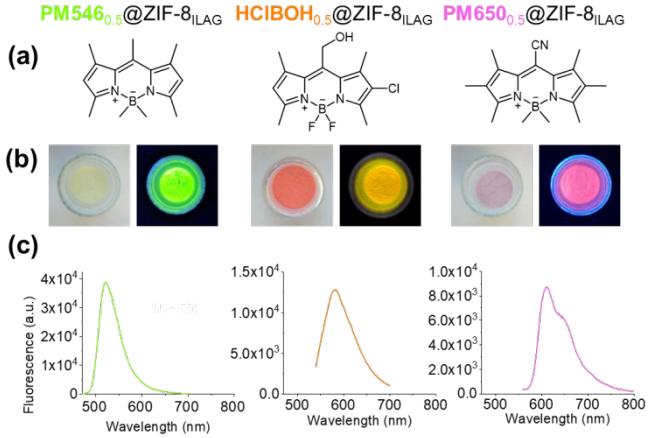

Figure 4. Preliminary results on the incorporation of other fluorescent BODIPY dyes into ZIF-8, using ILAG methodology. (a) Structures of BODIPY dyes (PM546, HClBOH,[72] and PM605). (b) BODIPY$_{0.5}$@ZIF-8$_{ILAG}$ powders under visible light (left) and UV-light (right) exposure. (c) Emission spectra of corresponding BODIPY$_{0.5}$@ZIF-8$_{ILAG}$ samples.

One may thus conceive mixtures suitable for white light emission. Given that encapsulated PM605 molecules are capable of undergoing through-pore energy transfer within ZIF-8 at high loadings, one may also conceive the development of solid-state materials for energy harvesting applications.

ASSOCIATED CONTENT

Supporting Information

The Supporting Information is available free of charge on the ACS Publications website. Materials and experimental methods, Supplementary Tables S1-S3, and Supplementary Figures S1-S15 (PDF).

AUTHOR INFORMATION

Corresponding Author

*E-mail: tomislav.friscic@mcgill.ca
*E-mail: gonzalo.cosa@mcgill.ca

Author Contributions

All authors contributed to data acquisition and analysis.

Notes

The authors declare no competing financial interests.

ACKNOWLEDGMENT

We thank the NSERC Discovery Grant (RGPIN-2017-06467), NSERC E. W. R. Steacie Memorial Fellowship (SMFSU 507347-17), NSERC Strategic Project Grant (STPGP 463405-14) the Fonds de Recherche du Quebec – Nature et Technologie (FQRNT), and the Canadian Foundation for Innovation (CFI) for funding. V.G. is thankful to the Drug Discovery and Training Program, Groupe de Recherche Axé sur la Structure des Protéines (GRASP), and NSERC Bionanomachines programs for postgraduate scholarships. AMD is helpful to the Drug Discovery and Training Program. We acknowledge Mr. David Morris and Aleksandra Djurić for help in acquiring BET data. We thank Prof. Dmytro Perepichka and Mr. Ehsan Hamzehpoor for access to fluorescence quantum yield measurements.

REFERENCES

1. Zhu, X.-H.; Peng, J.; Cao, Y.; Roncali, J. Solution-processable single-material molecular emitters for organic light-emitting devices. *Chem. Soc. Rev.* **2011**, *40*, 3509-3524.
2. Cicoira, F.; Santato, C. Organic Light Emitting Field Effect Transistors: Advances and Perspectives. *Adv. Funct. Mater.* **2007**, *17*, 3421-3434.
3. Hide, F.; Díaz-García, M. A.; Schwartz, B. J.; Andersson, M. R.; Pei, Q.; Heeger, A. J. Semiconducting Polymers: A New Class of Solid-State Laser Materials. *Science* **1996**, *273*, 1833-1836.
4. Samuel, I. D. W.; Turnbull, G. A. Organic Semiconductor Lasers. *Chem. Rev.* **2007**, *107*, 1272-1295.
5. Kumar, K.; Duan, H.; Hegde, R. S.; Koh, S. C. W.; Wei, J. N.; Yang, J. K. W. Printing colour at the optical diffraction limit. *Nat. Nanotechnol.* **2012**, *7*, 557-561.
6. Lu, Y.; Zhao, J.; Zhang, R.; Liu, Y.; Liu, D.; Goldys, E. M.; Yang, X.; Xi, P.; Sunna, A.; Lu, J.; Shi, Y.; Leif, R. C.; Huo, Y.; Shen, J.; Piper, J. A.; Robinson, J. P.; Jin, D. Tunable lifetime multiplexing using luminescent nanocrystals. *Nat. Photon.* **2013**, *8*, 32.
7. Basabe-Desmonts, L.; Reinhoudt, D. N.; Crego-Calama, M. Design of fluorescent materials for chemical sensing. *Chem. Soc. Rev.* **2007**, *36*, 993-1017.
8. Martínez-Máñez, R.; Sancenón, F. Fluorogenic and Chromogenic Chemosensors and Reagents for Anions. *Chem. Rev.* **2003**, *103*, 4419-4476.
9. Wolfbeis, O. S. An overview of nanoparticles commonly used in fluorescent bioimaging. *Chem. Soc. Rev.* **2015**, *44*, 4743-4768.
10. Birks, J. B. Excimers and Exciplexes. *Nature* **1967**, *214*, 1187-1190.
11. Birks, J. B. *Photophysics of aromatic molecules* **1970**, *Wily-Interscience, London*, 528-537.
12. Loudet, A.; Burgess, K. BODIPY Dyes and Their Derivatives: Syntheses and Spectroscopic Properties. *Chem. Rev.* **2007**, *107*, 4891-4932.
13. Shuzhang, X.; Qiong, C.; Feijun, D. Solid-Emissive BODIPY Derivatives: Design, Synthesis and Applications. *Curr. Org. Chem.* **2012**, *16*, 2970-2981.
14. Xi, H.; Yuan, C.-X.; Li, Y.-X.; Liu, Y.; Tao, X.-T. Crystal structures and solid-state fluorescence of BODIPY dyes based on [capital Lambda]-shaped Troger's base. *CrystEngComm* **2012**, *14*, 2087-2093.
15. Zhang, D.; Wen, Y.; Xiao, Y.; Yu, G.; Liu, Y.; Qian, X. Bulky 4-tritylphenylethynyl substituted boradiazaindacene: pure red emission, relatively large Stokes shift and inhibition of self-quenching. *ChemComm* **2008**, 4777-4779.
16. Vu, T. T.; Badré, S.; Dumas-Verdes, C.; Vachon, J.-J.; Julien, C.; Audebert, P.; Senotrusova, E. Y.; Schmidt, E. Y.; Trofimov, B. A.; Pansu, R. B.; Clavier, G.; Méallet-Renault, R. New Hindered BODIPY Derivatives: Solution and Amorphous State Fluorescence Properties. *J. Phys. Chem. C* **2009**, *113*, 11844-11855.
17. Vu, T. T.; Dvorko, M.; Schmidt, E. Y.; Audibert, J.-F.; Retailleau, P.; Trofimov, B. A.; Pansu, R. B.; Clavier, G.; Méallet-Renault, R. Understanding the Spectroscopic Properties and Aggregation Process of a New Emitting Boron Dipyrromethene (BODIPY). *J. Phys. Chem. C* **2013**, *117*, 5373-5385.
18. Ozdemir, T.; Atilgan, S.; Kutuk, I.; Yildirim, L. T.; Tulek, A.; Bayindir, M.; Akkaya, E. U. Solid-State Emissive BODIPY Dyes with Bulky Substituents As Spacers. *Org. Lett.* **2009**, *11*, 2105-2107.
19. Fu, G.-L.; Pan, H.; Zhao, Y.-H.; Zhao, C.-H. Solid-state emissive triarylborane-based BODIPY dyes: Photophysical properties and fluorescent sensing for fluoride and cyanide ions. *Org. Biomol. Chem.* **2011**, *9*, 8141-8146.

20. Lu, H.; Wang, Q.; Gai, L.; Li, Z.; Deng, Y.; Xiao, X.; Lai, G.; Shen, Z. Tuning the solid-state luminescence of BODIPY derivatives with bulky arylsilyl groups: synthesis and spectroscopic properties. *Chemistry* **2012**, *18*, 7852-61.

21. Yu. Schmidt, E.; Zorina, N. V.; Yu. Dvorko, M.; Protsuk, N. I.; Belyaeva, K. V.; Clavier, G.; Méallet-Renault, R.; Vu, T. T.; Mikhaleva, A. b. I.; Trofimov, B. A. A General Synthetic Strategy for the Design of New BODIPY Fluorophores Based on Pyrroles with Polycondensed Aromatic and Metallocene Substituents. *Chem. Eur. J.* **2011**, *17*, 3069-3073.

22. Schmidt, E. Y.; Trofimov, B. A.; Mikhaleva, A. b. I.; Zorina, N. V.; Protzuk, N. I.; Petrushenko, K. B.; Ushakov, I. A.; Dvorko, M. Y.; Méallet-Renault, R.; Clavier, G.; Vu, T. T.; Tran, H. T. T.; Pansu, R. B. Synthesis and Optical Properties of 2-(Benzo[b]thiophene-3-yl)pyrroles and a New BODIPY Fluorophore (BODIPY=4,4-Difluoro-4-bora-3a,4a-diaza-s-indacene). *Chem. Eur. J.* **2009**, *15*, 5823-5830.

23. Kubota, Y.; Uehara, J.; Funabiki, K.; Ebihara, M.; Matsui, M. Strategy for the increasing the solid-state fluorescence intensity of pyrromethene–BF2 complexes. *Tetrahedron Lett.* **2010**, *51*, 6195-6198.

24. Hu, R.; Lager, E.; Aguilar-Aguilar, A.; Liu, J.; Lam, J. W. Y.; Sung, H. H. Y.; Williams, I. D.; Zhong, Y.; Wong, K. S.; Peña-Cabrera, E.; Tang, B. Z. Twisted Intramolecular Charge Transfer and Aggregation-Induced Emission of BODIPY Derivatives. *J. Phys. Chem. C* **2009**, *113*, 15845-15853.

25. Tao, T.; Wang, S.-R.; Chen, L.; Qiu, H.; Xu, J.; Chen, M.-D. Synthesis and aggregation-induced emission of a pyrene decorated chiral BODIPY chromophore. *Inorg. Chem. Commun.* **2015**, *62*, 67-70.

26. Choi, S.; Bouffard, J.; Kim, Y. Aggregation-induced emission enhancement of a meso-trifluoromethyl BODIPY via J-aggregation. *Chem. Sci.* **2014**, *5*, 751-755.

27. Li, Q.; Qian, Y. Aggregation-induced emission enhancement and cell imaging of a novel (carbazol-N-yl)triphenylamine-BODIPY. *New J. Chem.* **2016**, *40*, 7095-7101.

28. Pérez-Ojeda, M. E.; Martín, V.; Costela, A.; García-Moreno, I.; Arroyo Córdoba, I. J.; Peña-Cabrera, E. Unprecedented solid-state laser action from BODIPY dyes under UV-pumping radiation. *Appl. Phys. B* **2012**, *106*, 911-914.

29. Wittmershaus, B. P.; Skibicki, J. J.; McLafferty, J. B.; Zhang, Y.-Z.; Swan, S. Spectral Properties of Single BODIPY Dyes in Polystyrene Microspheres and in Solutions. *J. Fluoresc.* **2001**, *11*, 119-128.

30. Zhu, M.; Jiang, L.; Yuan, M.; Liu, X.; Ouyang, C.; Zheng, H.; Yin, X.; Zuo, Z.; Liu, H.; Li, Y. Efficient tuning nonlinear optical properties: Synthesis and characterization of a series of novel poly(aryleneethynylene)s co-containing BODIPY. *J. Polym. Sci. A Polym. Chem.* **2008**, *46*, 7401-7410.

31. Nagai, A.; Kokado, K.; Miyake, J.; Chujo, Y. Highly Luminescent Nanoparticles: Self-Assembly of Well-Defined Block Copolymers by π−π Stacked BODIPY Dyes as Only a Driving Force. *Macromolecules* **2009**, *42*, 5446-5452.

32. Monguzzi, A.; Ballabio, M.; Yanai, N.; Kimizuka, N.; Fazzi, D.; Campione, M.; Meinardi, F. Highly Fluorescent Metal–Organic-Framework Nanocomposites for Photonic Applications. *Nano Lett.* **2018**, *18*, 528-534.

33. Beldon, P. J.; Fábián, L.; Stein, R. S.; Thirumurugan, A.; Cheetham, A. K.; Friščić, T. Rapid Room-Temperature Synthesis of Zeolitic Imidazolate Frameworks by Using Mechanochemistry. *Angew. Chem. Int. Ed.* **2010**, *49*, 9640-9643.

34. Friscic, T.; Fabian, L. Mechanochemical conversion of a metal oxide into coordination polymers and porous frameworks using liquid-assisted grinding (LAG). *CrystEngComm* **2009**, *11*, 743-745.

35. Cliffe, M. J.; Mottillo, C.; Stein, R. S.; Bucar, D.-K.; Friscic, T. Accelerated aging: a low energy, solvent-free alternative to solvothermal and mechanochemical synthesis of metal-organic materials. *Chem. Sci.* **2012**, *3*, 2495-2500.

36. Mottillo, C.; Lu, Y.; Pham, M.-H.; Cliffe, M. J.; Do, T.-O.; Friscic, T. Mineral neogenesis as an inspiration for mild, solvent-free synthesis of bulk microporous metal-organic frameworks from metal (Zn, Co) oxides. *Green Chem.* **2013**, *15*, 2121-2131.

37. Sumida, K.; Rogow, D. L.; Mason, J. A.; McDonald, T. M.; Bloch, E. D.; Herm, Z. R.; Bae, T.-H.; Long, J. R. Carbon Dioxide Capture in Metal–Organic Frameworks. *Chem. Rev.* **2012**, *112*, 724-781.

38. Denny Jr, M. S.; Moreton, J. C.; Benz, L.; Cohen, S. M. Metal–organic frameworks for membrane-based separations. *Nat. Rev. Mater.* **2016**, *1*, 16078.

39. Simmons, J. M.; Wu, H.; Zhou, W.; Yildirim, T. Carbon capture in metal-organic frameworks-a comparative study. *Energy Environ. Sci.* **2011**, *4*, 2177-2185.

40. Dhakshinamoorthy, A.; Alvaro, M.; Garcia, H. Commercial metal-organic frameworks as heterogeneous catalysts. *ChemComm* **2012**, *48*, 11275-11288.

41. Banerjee, R.; Phan, A.; Wang, B.; Knobler, C.; Furukawa, H.; O'Keeffe, M.; Yaghi, O. M. High-Throughput Synthesis of Zeolitic Imidazolate Frameworks and Application to CO₂ Capture. *Science* **2008**, *319*, 939-943.

42. Tansell, A. J.; Jones, C. L.; Easun, T. L. MOF the beaten track: unusual structures and uncommon applications of metal–organic frameworks. *Chem. Cent. J.* **2017**, *11*, 100.

43. Zhang, J.-P.; Zhang, Y.-B.; Lin, J.-B.; Chen, X.-M. Metal Azolate Frameworks: From Crystal Engineering to Functional Materials. *Chem. Rev.* **2012**, *112*, 1001-1033.

44. Park, K. S.; Ni, Z.; Côté, A. P.; Choi, J. Y.; Huang, R.; Uribe-Romo, F. J.; Chae, H. K.; O'Keeffe, M.; Yaghi, O. M. Exceptional chemical and thermal stability of zeolitic imidazolate frameworks. *Proc. Natl. Acad. Sci. U.S.A.* **2006**, *103*, 10186-10191.

45. Huang, X.-C.; Lin, Y.-Y.; Zhang, J.-P.; Chen, X.-M. Ligand-Directed Strategy for Zeolite-Type Metal–Organic Frameworks: Zinc(II) Imidazolates with Unusual Zeolitic Topologies. *Angew. Chem. Int. Ed.* **2006**, *45*, 1557-1559.

46. Wen, Y.; Sheng, T.; Zhu, X.; Zhuo, C.; Su, S.; Li, H.; Hu, S.; Zhu, Q.-L.; Wu, X. Introduction of Red-Green-Blue Fluorescent Dyes into a Metal–Organic Framework for Tunable White Light Emission. *Adv. Mater.* **2017**, *29*, 1700778.

47. Yan, D.; Tang, Y.; Lin, H.; Wang, D. Tunable Two-color Luminescence and Host–guest Energy Transfer of Fluorescent Chromophores Encapsulated in Metal-Organic Frameworks. *Sci. Rep.* **2014**, *4*, 4337.

48. Wang, C.; Tian, L.; Zhu, W.; Wang, S.; Wang, P.; Liang, Y.; Zhang, W.; Zhao, H.; Li, G. Dye@bio-MOF-1 Composite as a Dual-Emitting Platform for Enhanced Detection of a Wide Range of Explosive Molecules. *ACS Appl. Mater. Interfaces* **2017**, *9*, 20076-20085.

49. Han, T.-T.; Yang, J.; Liu, Y.-Y.; Ma, J.-F. Rhodamine 6G loaded zeolitic imidazolate framework-8 (ZIF-8) nanocomposites for highly selective luminescent sensing of Fe3+, Cr6+ and aniline. *Microporous Mesoporous Mater.* **2016**, *228*, 275-288.

50. Morabito, J. V.; Chou, L.-Y.; Li, Z.; Manna, C. M.; Petroff, C. A.; Kyada, R. J.; Palomba, J. M.; Byers, J. A.; Tsung, C.-K. Molecular Encapsulation beyond the Aperture Size Limit through Dissociative Linker Exchange in Metal–Organic Framework Crystals. *J. Am. Chem. Soc.* **2014**, *136*, 12540-12543.

51. Li, Z.; Rayder, T. M.; Luo, L.; Byers, J. A.; Tsung, C.-K. Aperture-Opening Encapsulation of a Transition Metal Catalyst in a Metal–Organic Framework for CO2 Hydrogenation. *J. Am. Chem. Soc.* **2018**, *140*, 8082-8085.

52. Wang, T.; Li, S.; Zou, Z.; Hai, L.; Yang, X.; Jia, X.; Zhang, A.; He, D.; He, X.; Wang, K. A zeolitic imidazolate framework-8-based indocyanine green theranostic agent for infrared fluorescence imaging and photothermal therapy. *J. Mater. Chem. B* **2018**, *6*, 3914-3921.

53. Zheng, H.; Zhang, Y.; Liu, L.; Wan, W.; Guo, P.; Nyström, A. M.; Zou, X. One-pot Synthesis of Metal–Organic Frameworks with Encapsulated Target Molecules and Their Applications for Controlled Drug Delivery. *J. Am. Chem. Soc.* **2016**, *138*, 962-968.

54. Lu, G.; Li, S.; Guo, Z.; Farha, O. K.; Hauser, B. G.; Qi, X.; Wang, Y.; Wang, X.; Han, S.; Liu, X.; DuChene, J. S.; Zhang, H.; Zhang, Q.; Chen, X.; Ma, J.; Loo, S. C. J.; Wei, W. D.; Yang, Y.; Hupp, J. T.; Huo, F. Imparting functionality to a metal–organic framework material by controlled nanoparticle encapsulation. *Nat. Chem.* **2012**, *4*, 310-316.

55. López-Domínguez, P.; López-Periago, A. M.; Fernández-Porras, F. J.; Fraile, J.; Tobias, G.; Domingo, C. Supercritical CO2 for the synthesis of nanometric ZIF-8 and loading with hyperbranched aminopolymers. Applications in CO2 capture. *J. CO2 Util.* **2017**, *18*, 147-155.

56. Nune, S. K.; Thallapally, P. K.; Dohnalkova, A.; Wang, C.; Liu, J.; Exarhos, G. J. Synthesis and properties of nano zeolitic imidazolate frameworks. *ChemComm* **2010**, *46*, 4878-4880.

57. Venna, S. R.; Carreon, M. A. Highly Permeable Zeolite Imidazolate Framework-8 Membranes for CO2/CH4 Separation. *J. Am. Chem. Soc.* **2010**, *132*, 76-78.

58. Fairen-Jimenez, D.; Moggach, S. A.; Wharmby, M. T.; Wright, P. A.; Parsons, S.; Düren, T. Opening the Gate: Framework Flexibility in ZIF-8 Explored by Experiments and Simulations. *J. Am. Chem. Soc.* **2011**, *133*, 8900-8902.

59. Cravillon, J.; Schröder, C. A.; Bux, H.; Rothkirch, A.; Caro, J.; Wiebcke, M. Formate modulated solvothermal synthesis of ZIF-8 investigated using time-resolved in situ X-ray diffraction and scanning electron microscopy. *CrystEngComm* **2012**, *14*, 492-498.

60. Kida, K.; Okita, M.; Fujita, K.; Tanaka, S.; Miyake, Y. Formation of high crystalline ZIF-8 in an aqueous solution. *CrystEngComm* **2013**, *15*, 1794-1801.

61. Kolmykov, O.; Commenge, J.-M.; Alem, H.; Girot, E.; Mozet, K.; Medjahdi, G.; Schneider, R. Microfluidic reactors for the size-controlled synthesis of ZIF-8 crystals in aqueous phase. *Mater. Des.* **2017**, *122*, 31-41.

62. Krumova, K.; Oleynik, P.; Karam, P.; Cosa, G. Phenol-Based Lipophilic Fluorescent Antioxidant Indicators: A Rational Approach. *J. Org. Chem.* **2009**, *74*, 3641-3651.

63. Eggeling, C.; Widengren, J.; Rigler, R.; Seidel, C. A. M., Photostability of Fluorescent Dyes for Single-Molecule Spectroscopy: Mechanisms and Experimental Methods for Estimating Photobleaching in Aqueous Solution. In *Applied Fluorescence in Chemistry, Biology and Medicine*, Springer Berlin Heidelberg: Berlin, Heidelberg, 1999; pp 193-240.

64. Guether, R.; Reddington, M. V. Photostable Cyanine Dye β-Cyclodextrin Conjugates. *Tetrahedron Lett.* **1997**, *38*, 6167-6170.

65. Mohanty, J.; Nau, W. M. Ultrastable Rhodamine with Cucurbituril. *Angew. Chem. Int. Ed.* **2005**, *44*, 3750-3754.

66. Yang, S. K.; Shi, X.; Park, S.; Doganay, S.; Ha, T.; Zimmerman, S. C. Monovalent, Clickable, Uncharged, Water-Soluble Perylenediimide-Cored Dendrimers for Target-Specific Fluorescent Biolabeling. *J. Am. Chem. Soc.* **2011**, *133*, 9964-9967.

67. Yang, S. K.; Zimmerman, S. C. Polyglycerol-Dendronized Perylenediimides as Stable, Water-Soluble Fluorophores. *Adv. Funct. Mater.* **2012**, *22*, 3023-3028.

68. Heek, T.; Fasting, C.; Rest, C.; Zhang, X.; Wurthner, F.; Haag, R. Highly fluorescent water-soluble polyglycerol-dendronized perylene bisimide dyes. *ChemComm* **2010**, *46*, 1884-1886.

69. Yang, S. K.; Shi, X.; Park, S.; Ha, T.; Zimmerman, S. C. A dendritic single-molecule fluorescent probe that is monovalent, photostable and minimally blinking. *Nat. Chem.* **2013**, *5*, 692-697.

70. Redy-Keisar, O.; Huth, K.; Vogel, U.; Lepenies, B.; Seeberger, P. H.; Haag, R.; Shabat, D. Enhancement of fluorescent properties of near-infrared dyes using clickable oligoglycerol dendrons. *Org. Biomol. Chem.* **2015**, *13*, 4727-4732.

71. Zlotea, C.; Campesi, R.; Cuevas, F.; Leroy, E.; Dibandjo, P.; Volkringer, C.; Loiseau, T.; Férey, G.; Latroche, M. Pd Nanoparticles Embedded into a Metal-Organic Framework: Synthesis, Structural Characteristics, and Hydrogen Sorption Properties. *J. Am. Chem. Soc.* **2010**, *132*, 2991-2997.

72. Krumova, K.; Cosa, G. Bodipy Dyes with Tunable Redox Potentials and Functional Groups for Further Tethering: Preparation, Electrochemical, and Spectroscopic Characterization. *J. Am. Chem. Soc.* **2010**, *132*, 17560-17569.

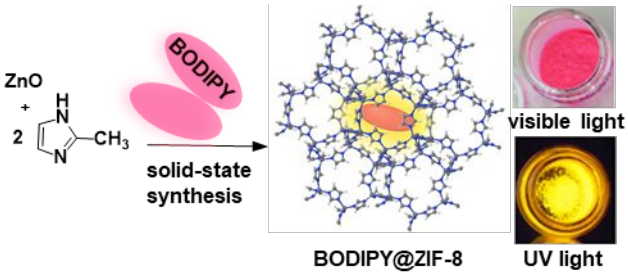
ZnO
+
2
H
N
N
CH3
BODIPY
solid-state
synthesis
visible light
UV light
BODIPY@ZIF-8